Using chaotic advection to enhance the continuous heat-hold-cool sterilisation process

Tian, Shuai; Barigou, Mostafa

DOI:
10.1016/j.ifset.2016.03.007

Document Version
Peer reviewed version

Citation for published version (Harvard):
Tian, S & Barigou, M 2016, 'Using chaotic advection to enhance the continuous heat-hold-cool sterilisation process', *Innovative Food Science and Emerging Technologies*, vol. 34, pp. 352-366. https://doi.org/10.1016/j.ifset.2016.03.007

Using chaotic advection to enhance the continuous heat-hold-cool sterilisation process

Shuai Tian, Mostafa Barigou

PII: S1466-8564(16)30039-X
DOI: doi: 10.1016/j.ifset.2016.03.007
Reference: INNFOO 1495

To appear in: *Innovative Food Science and Emerging Technologies*

Received date: 11 January 2016
Revised date: 15 March 2016
Accepted date: 16 March 2016

Please cite this article as: Tian, S. & Barigou, M., Using chaotic advection to enhance the continuous heat-hold-cool sterilisation process, *Innovative Food Science and Emerging Technologies* (2016), doi: 10.1016/j.ifset.2016.03.007

USING CHAOTIC ADVECTION TO ENHANCE THE CONTINUOUS HEAT-HOLD-COOL STERILISATION PROCESS

Shuai Tian and Mostafa Barigou*

School of Chemical Engineering, University of Birmingham, Edgbaston, Birmingham, B15 2TT, UK

Abstract

In a conventional continuous sterilisation process, the food product flows steadily through a heat-hold-cool system, but viscous flow poses a serious challenge as heat transfer is controlled by thermal conduction which leads to a wide radial temperature distribution and slow heating of the core region of the flow. We use a validated Computational Fluid Dynamics (CFD) model to show that the superimposition of transverse mechanical oscillations on the heat-hold-cool sterilisation process of a viscous single-phase Newtonian fluid, creates a strong oscillatory-perturbed or chaotic advection flow which leads to significant improvements in thermal processing uniformity and product quality compared with a conventional process with or without an inline static mixer fitted. Chaotic advection flow produces processing conditions which are more in line with the high temperature for short time (HTST) assumption. Results show that the vibrated process leads to faster nearly-uniform heating and cooling, thus, achieving much higher levels of sterility and product quality in a much shorter process.

Industrial Relevance

Technological solutions are needed to help solve the long-standing problem of wide variation of product sterility and nutritional quality across the tube in continuous thermal processing of viscous fluids, where much of the product has to be over-processed to ensure sterility throughout, thus, often violating the high temperature for short time (HTST) processing assumption. Superimposing a secondary chaotic flow on the process leads to high levels of sterility, processing uniformity and product quality over relatively short process lengths. This represents an enhanced process which surpasses conventional steady flow sterilisation even when an usually undesirable static mixer is fitted.

Keywords: CFD, chaotic advection, continuous sterilisation, food quality, food sterility, vibration, viscous flow.

*Corresponding author: Tel: +44 (0)121 414 5277 Fax: +44 (0)121 414 5324 Email: m.barigou@bham.ac.uk

1. Introduction

Cooking is a critical step in most food manufacturing processes. Thermal processing brings about irreversible changes in food textural and sensory properties, whilst at the same time achieving the desired level of microbial sterility. It is not possible nor is it necessary to eliminate all viable organisms from the material. Organoleptic and nutritive properties of foods are adversely affected by heat, and the process must only be as severe as necessary to ensure commercial sterility. Spore reduction and nutrient loss are governed by different kinetics, the rates of which are dictated by the processing conditions. A food that is optimally cooked would be safe but would also have sensory and nutritious properties that are most acceptable to the consumer. The optimisation of such thermal treatments poses a challenging manufacturing problem (Barigou *et al.*, 1998). The overriding importance of food safety often results in the food being exposed to a more severe process than is desirable from a quality aspect, resulting in lower sensory and nutritional attributes, especially with sensitive products, than is actually possible.

In continuous aseptic processing, a food mixture passes continuously through a heat-hold-cool system, and is then packaged in pre-sterilised containers (Holdsworth, 1992; David *et al.*, 2012). The food is heated to the required temperature in the heating stage, is then held at such a temperature in an insulated tube for long enough to ensure that the required level of sterility has been attained, and is then cooled to typically ambient temperature. Most foodstuffs tend to be viscous (e.g., soups, sauces) and in general flow occurs in the laminar regime. In a tubular heat exchanger, radial laminar heat transfer is governed essentially by slow thermal conduction which leads to a wide radial temperature distribution that poses a serious challenge in such manufacturing processes. In continuous food sterilisation, the non-uniform velocity profile which characterises viscous flow coupled with a non-uniform temperature distribution means that the coldest parts of the fluid at the centre of the tube travel the fastest, thus, resulting in a wide variation of product sterility and nutritional quality across the tube. The output conditions will be a mixture of fluid at different radial positions. The challenge is to be able to sterilise the fastest parts in the core region of the tube without over-processing too much the slowest parts near the wall. Increasing the temperature of the inner regions of the fluid is highly desirable so that ideally all parts of the fluid receive equal thermal treatment. Furthermore, better uniformity in the temperature profile helps reduce local variations in the fluid rheological properties which cause distortions in the velocity profile, thus making the flow behaviour of the fluid more predictable, especially in the case of complex non-Newtonian food rheology. Another aspect that should be considered in the design of such processes is the contribution of

the cooling stage to product sterilisation. The product leaving the holding tube will cool at a finite rate and some reaction leading to microbial lethality must occur. Conservative approaches tend to ignore this contribution. An optimal process design should take into account all contributions to lethality from the heating, holding and cooling stages (Barigou *et al.*, 1998).

The microbiological lethality delivered to the product and the extent to which product quality is preserved is a function of the residence time of the product in the sterilisation process as well as the temperatures to which it is exposed. This must be taken into account when designing a continuous heat preservation process. To calculate the length of the process, conservative design rules usually assume that all of the fluid flows at twice the mean velocity (i.e. the maximum centreline velocity in Newtonian flow) to ensure complete product sterility. Whilst, this ensures sterility, such an assumption results in poor sensory and nutritional attributes, especially with sensitive products. A good process design should aim at achieving a narrow residence time distribution and coupling safety assurance with quality optimisation, so that the process delivers the necessary microbial lethality to the slowest heating zones of the flow whilst not over-processing any significant amounts of the product.

To improve the uniformity of the temperature distribution, methods of increasing radial mixing are required. This problem has been recognised for a long time but effective technological solutions are still missing. Radial mixing can be achieved by turbulent flow conditions but the usually high fluid viscosities encountered in practice make this proposition often impractical and/or uneconomical. Chaotic advection, however, is an alternative to turbulence, and uses the stretching and folding property of chaotic flows to promote fluid mixing at low Reynolds numbers. Various ways have been proposed in the engineering literature to improve heat convection by using Dean vortex generators (Chagny *et al.*, 2000) or adding internal screw-thread structures on the wall to disrupt the boundary layer (Shrirao *et al.*, 2013), but such technological solutions are limited by their manufacturing complexity, cost, their high proneness to fouling and clogging, and the difficulty to keep them clean. Similarly, inserts or inline static mixers are used to promote radial fluid mixing and a number of designs exist (Hobbs and Muzzio, 1997; Saatdjian *et al.*, 2012a). In viscous flow, such devices can achieve a high degree of fluid mixing but usually at the expense of a high pressure drop. However, these inserts too are generally prohibited in hygienic processes because of the risk of contamination as their complex geometries also promote fouling and make them difficult to clean. A number of studies have also demonstrated the effects of

pulsating flow on the heat flux and Nusselt number in tubes (Gundogdu and Carpinlioglu, 1999). However, its effectiveness in achieving a uniform radial temperature distribution in viscous fluids has not been reported.

We recently reported on a novel technique which combines transverse mechanical oscillations with a stepwise angular change of oscillation orientation to generate a strong oscillatory-perturbed or chaotic flow in a heating tube, which achieves a high degree of radial fluid mixing, thermal boundary layer development, temperature uniformity and heat transfer in viscous tube flow (Tian and Barigou, 2015; Eesa and Barigou 2010, 2011). In this paper, we extend this work to demonstrate the large positive effects that such a technique can have on the thermal processing of a viscous single-phase fluid in a continuous heat-hold-cool sterilisation process, and the potential for achieving high temperature for short time (HTST) processing, a long-standing problem in food sterilisation. The performance of the technique is compared to traditional heat-hold-cool processing with and without the use of an inline Kenics static mixer. The Kenics mixer is widely used in industry and has been well characterized in the literature. It is one of the low pressure drop designs and it has been reported that flow division, flow reversal and radial mixing all contribute to the performance of the Kenics mixer (Saatdjian, E. *et al*., 2012b; Godfrey, J.C., 2000).

2. Theory

2.1 Temperature-dependent fluid viscosity model

The single-phase fluid used is an incompressible, temperature-dependent Newtonian fluid whose viscosity is assumed constant at a given temperature and is described by the well-known Arrhenius relationship:

$$\mu = k_0 exp\left(\frac{E_a}{R_g T}\right) \tag{1}$$

where k_0 is a pre-exponential factor, R_g is the ideal gas constant, T is temperature and E_a is the activation energy for viscosity. The constants k_0 and E_a are determined experimentally and their values for various fluids have been reported in the literature (Steffe, 1996). These parameters, as well as other physical properties (density ρ, specific heat capacity C_p, and thermal conductivity λ) were assumed constant and their values are given in Table1.

2.2 Transverse harmonic motion

In its basic form (**VF**), the technique uses transverse mechanical oscillations imposed on the tube wall in a direction perpendicular to the tube axis, as illustrated in Figure 1(*c*), and the wall displacement *x* is described by the harmonic function:

$$x = A\sin(\omega t) \tag{2}$$

where *A* is the amplitude of vibration, *t* is time, and ω is the angular function of the frequency of vibration, *f*, such that $\omega = 2\pi f$. The linear transversal velocity of the tube wall is then:

$$u = \frac{dx}{dt} = A\omega\cos(\omega t) \tag{3}$$

In the new enhanced form of the technique (**VF-SR**), the tube is continuously oscillated transversally but the orientation of oscillation is rotated instantly in a stepwise manner by an angle of 45 degrees about the tube axis, as depicted in Figure 1(*d*). The time interval, Δt, between change of orientation steps, needs to be optimized for a given set of process conditions. For the conditions considered in this work, a value $\Delta t \sim 10$ s was determined by numerical experimentation, thus, the frequency of the step rotation, Ω, is (and is expected to always be) very low compared with the frequency of lateral oscillations; for example, in this case $\Omega = 0.1$ Hz compared to $f = 50$ Hz. The effects of Ω on the thermal process are further discussed below.

Under steady state, the flow regime was always laminar with a Reynolds number ($Re = \rho\overline{w}D/\mu$) within the range 1.4 – 90, where *D* is tube diameter and $\overline{w}$ is mean axial velocity. When the tube was vibrated, the vibration Reynolds number $\left(Re_v = \frac{\rho A\omega D}{\mu}\right)$ was within the range 22 – 1400; so flow remained laminar under all conditions of flow and temperature.

2.3 Criterion for chaotic advection

Chaotic advection flow is known to exist when an infinitely small initial deviation in the position of a fluid trajectory will lead to exponential divergence with time. To show that the superimposed transverse oscillations generate chaotic advection flow, we estimate the Lyapunov exponent, a quantity that characterises the rate of separation of infinitesimally close trajectories (Kantz and Schreiber, 2004). The rate of separation can be different for different orientations of the initial separation vector. Thus, there is a spectrum of Lyapunov exponents, λ, defined as:

$$Dis(t) \approx \mathrm{e}^{\lambda t}(Dis_{t=0}) \tag{4}$$

where *Dis* is the instantaneous separation distance between trajectories and λ is given by:

$$\lambda = \lim_{t\to\infty} \lim_{Dis_{t=0}\to 0} \frac{Dis(t)}{Dis_{t=0}} \tag{5}$$

A positive maximum Lyapunov exponent is usually taken as an indication that the system is chaotic.

2.4 Governing equations

The governing transport equations which are the basis of the CFD model can be written in their general form (Bird *et al.*, 1987), thus:

Continuity: $$\nabla \cdot \boldsymbol{U} = 0 \tag{6}$$

Momentum: $$\rho \frac{\mathrm{D}\boldsymbol{U}}{\mathrm{D}t} = -\nabla p + \nabla^2 \mu \boldsymbol{U} + \rho \boldsymbol{g} \tag{7}$$

Energy: $$\rho C_p \frac{\mathrm{D}T}{\mathrm{D}t} = \lambda \nabla^2 T + \mu \dot{\gamma}^2 \tag{8}$$

where p is fluid pressure, $\boldsymbol{g}$ is gravitational acceleration, $\boldsymbol{U}$ is the velocity field and $\dot{\gamma}$ is the second invariant of the shear rate tensor, defined as $\dot{\gamma} \equiv \left[\frac{1}{2}(\dot{\gamma}:\dot{\gamma})\right]^{\frac{1}{2}}$.

2.5 In-flow sterility and quality

Food sterility and quality levels can be calculated using the standard Eqs. (9) and (10), respectively:

$$F = \int_0^t 10^{(T-T_{Fref})/z_F}\, dt \tag{9}$$

where, F which is known as the F-value, is an equivalent heating time for which the product could be held at a constant reference temperature, T_{Fref}, to give the same final concentration of microbial pathogens as a processing time, t, for which the temperature, T, changes. T_{Fref} depends on the organism being inactivated or the indicator organism used in the process, e.g. 121.1 °C for the pathogen *C. botulinum*, and z_F is the temperature change which produces a 10-fold change in reaction rate from the rate at the reference temperature, e.g. z_F = 10 °C for *C. botulinum* (Jung and Fryer, 1999).

Product quality loss is estimated using the cook value, C, also known as the C-value, a parameter defined in a similar way to the F-value, which gives a measure of the extent of nutrient loss in units of time:

$$C = \int_0^t 10^{(T-T_{Cref})/z_C}\, dt \tag{10}$$

where T_{Cref} is a reference temperature dependant on the nutrient under consideration, e.g. 121.1 °C, and z_C is the temperature change which produces a 10-fold change in reaction rate from the rate at the reference temperature, e.g. z_C = 48 °C for thiamine denaturation (Jung and Fryer, 1999).

2.6 Uniformity of radial distribution of in-flow sterility and quality

The coefficient of variation, C_v, is used as a measure of radial sterility and quality uniformity across the tube and is usually defined as the ratio of the standard deviation σ to the volume-weighted mean value $\bar{F}$ or $\bar{C}$. However, it should be noted that when the mean value is small, such a definition can lead to an artificially high value of C_v. To avoid such erroneous values, we use a modified coefficient of variation, such that for F:

$$C_{v\text{-}F} = \frac{\sigma_F}{\bar{F}-\bar{F}_{ideal}} \tag{11}$$

where $\bar{F}_{ideal}$ is the volume-weighted mean value achieved at a given axial position z of an ideal plug flow having the same inlet conditions of mean velocity and temperature as the real laminar flow.

The volume-flowrate weighted mean sterility across the tube, $\bar{F}$, is obtained by dividing the tube cross-section into a large number of cells (N = 1860), as shown in Figure 2, which can be identified by their polar coordinates r and θ. The analysis was conducted using this regular grid implemented in MATLAB to avoid the difficulties associated with the complex and varied cell shapes of the computational CFD grid. The local sterility and axial velocity in a given cell are denoted by $F(r,\theta)$ and $w(r,\theta)$, respectively, and are considered at their nearly constant time-average values reached after a vibration time equivalent to the fluid residence time in the tube. Thus, $\sum_{i=1}^{N} w(r,\theta)S(r,\theta) = Q$ represents the volumetric flowrate through a cell, where $S(r,\theta)$ is the cross-sectional area of the cell. The volume-flowrate weighted mean sterility is, therefore, given by:

$$\overline{F} = \frac{1}{Q}\sum_{i=1}^{N} F(r,\theta)w(r,\theta)S(r,\theta) \tag{12}$$

In the limit as $S(r,\theta) \to 0$, i.e. for large N, the uniformity of the sterility distribution over the tube cross-section can be well described by the standard deviation:

$$\sigma_F = \sqrt{\frac{1}{Q^2}\sum_{i=1}^{N}\left[F(r,\theta)w(r,\theta)S(r,\theta) - \overline{F}w(r,\theta)S(r,\theta)\right]^2} \tag{13}$$

and the coefficient of variation $C_{v\text{-}F}$ (Eq. 9).

The above relationships can be used to evaluate the standard deviation, σ_C, and coefficient of variation, $C_{v\text{-}C}$, for the quality, C. It should be noted, however, that in the cooling stage, $\bar{F}_{ideal} > \bar{F}$ and $\bar{C}_{ideal} > \bar{C}$, and therefore the absolute value $|\bar{F} - \bar{F}_{ideal}|$ or $|\bar{C} - \bar{C}_{ideal}|$ should be used in Eq. (11).

3. CFD model

3.1 Simulations

3.1.1 Geometries and meshing

Three-dimensional simulations were set up and executed using the commercial software package ANSYS Workbench 14.5. The flow geometries were created and meshed using the software ICEM, while flow specification, solving and post-processing were all performed using CFX 14.5. In its basic form, the geometry consisted of a straight tube 30 mm in diameter and 2400 mm in length with three surface boundaries: inlet, outlet, and wall (Figure 1(*a*)). The geometry was meshed with hexahedral cells, as shown in Figure 3(*a*). To optimise the mesh size it was necessary to carry out a mesh-independence study; this was done by performing a

number of simulations with different mesh sizes, starting from a coarse mesh and refining it until results were no longer dependent on the mesh size. The mesh thus achieved contained approximately 4000 hexahedral cells per centimetre of tube length and around 1000 cells across the tube section, giving a mesh size in the core region of about 1 mm. The mesh size near the wall was progressively reduced down to 0.1 mm to enhance mesh resolution in this region of high velocity and temperature gradients. The quality of the mesh measured by its orthogonality and warpage was over 0.75, well above the generally accepted minimum value of 0.4 for a good mesh.

Other simulations were conducted using the same setup with 48 segments of the helical Kenics static mixer inserted to fill the whole tube, as illustrated (SF-KM) in Figure 1(*b*). The mixer consists of left and right twisting helical elements with a standard length to diameter ratio of 1.5; detailed dimensions are given in Table 2. It should be noted that a mesh-independence study was conducted for each one of the flow geometries used. Similar to the other geometry, fine inflation layers of hexahedral cells were generated around the helical surfaces, so that the mesh was progressively reduced down to 0.15 mm at these surfaces and at the pipe wall to accurately capture the velocity and temperature gradients in these regions, as shown in Figure 3(*b*).

3.1.2 Boundary conditions

(i) Heating stage

In all simulations, a uniform temperature T_{in} = 20 °C and a mass flowrate $\dot{m} = 0.0281$ kg s^{-1} were specified at the heating tube inlet, and a zero gauge pressure was set at the outlet. The mass flowrate was chosen to give a mean flow velocity $\overline{w} = 4.0$ cm s^{-1}, which is typical of values used in the processing of viscous food materials (Steffe, 1996; Jung and Fryer, 1999). A constant uniform wall temperature and a no-slip condition were assigned at the heating tube wall. In continuous HTST food processing, wall temperatures as high as 180 °C are used in practice; here, T_w was set at 140 °C.

(ii) Holding stage

The temperature and velocity profiles at the exit of the heating stage were used as the inlet boundary conditions for the holding stage. In addition, the tube wall was specified as adiabatic with no-slip, and a zero gauge pressure was set at the tube outlet.

(iii) Cooling stage

Where a holding stage was used, unless otherwise stated, the temperature and velocity profiles at the exit section were used as the inlet boundary conditions for the cooling stage. A no-slip isothermal tube wall with T_w = 20 °C and a zero gauge pressure at the outlet was used.

Where a static mixer was used, the helical surface was assumed adiabatic. For vibratory flow in anyone of the above heat-hold-cool stages, a harmonic velocity function defined by Eq. (3) was applied at the tube wall and the mesh displacement was specified using Eq. (2).

3.1.3 Numerical scheme

The CFD code uses a finite-volume-based method to discretise the governing transport Eqs. (6), (7), (8). In this method, the variable value at an integration point, ϕ_{ip}, is calculated from the variable value at the upwind node, ϕ_{up}, and the variable gradient, $\nabla\phi$, thus:

$$\phi_{ip} = \phi_{up} + \beta\nabla\phi\Delta\boldsymbol{r} \tag{14}$$

where β is a blend factor and $\Delta\boldsymbol{r}$ is the vector from the upwind node to the integration point. With β = 0, the scheme is first order accurate and does not result in non-physical variable values. On the other hand, with β = 1, the scheme is second order accurate but it may result in non-physical values. In the so-called 'High Resolution Advection Scheme' implemented here, the value of β is calculated locally to be as close to 1 as possible without resulting in non-physical variable values (Barth and Jesperson, 1989). This scheme is therefore intended to satisfy the requirements of both accuracy and boundedness.

Simulations involving steady flow were conducted in the steady-state mode, whereas simulations of vibrational flow were conducted in the transient mode. For a transversely moving boundary, the mesh deformation option in CFX was used which allows the specification of the motion of nodes on boundary regions of the mesh. The motion of all remaining nodes is determined by the so-called displacement diffusion model which is designed to preserve the relative mesh distribution of the initial mesh.

The transient scheme used for the solution to march in time was the 'Second Order Backward Euler Scheme'. The simulation was solved over the entire mean residence time of the fluid which is determined by the tube

length and mean flow velocity. For example, for a tube length of 2400 mm and flow velocity of 4.0 cm s^{-1}, as used here, the mean fluid residence time in the tube is 60 s. This time duration was divided into equal time steps, the size of which (1.6667×10^{-3} s) was determined by dividing the vibration cycle into an optimised number of 12 equal time steps. Using a larger number of (smaller) time steps per vibration cycle did not change the simulation results but prolonged the simulations considerably; for example, halving the time step did not significantly improve accuracy but nearly doubled simulation time.

Convergence of the numerical solution was assumed when the root mean squares (RMS) of the residuals of mass, momentum and energy all reached 10^{-4} at each time step which is a good level of accuracy given the complexity of the problem. Achieving this level of convergence typically required 8-12 iterations per time step for vibrational flow and about 50 iterations for steady flow. In practice, however, most of the equations generally reached residual RMS values well below the specified target.

3.2 Sterility and quality profiles: Lagrangian particle tracking

In a continuous flow process, different fluid elements will have different thermal histories and will be subjected to different levels of microbial lethality. To calculate local values of sterility at the exit, a Lagragian particle tracking method was used. Thus, the function of one-way coupled particle tracking was implemented in the CFD code to predict fluid trajectories along the tube. Unlike two-way coupling (i.e. full coupling) which takes into account not only the effect of particles on continuous phase flow but also the influence of continuous phase flow on particles, one-way coupling simply predicts the particles' path lines as a post-process based on the computed flow field (Mostofa *et al.*, 2010; Jakobsen, 2014). One-way coupling does not allow particles to affect continuous phase flow and therefore gives a much more accurate tracking of fluid flow than full coupling. Thus, massless microscopic fluid particles (1 μm) were introduced at the tube inlet and their trajectories and, hence, their temperature and velocity histories, were recorded. Thus, these massless particles are assumed to faithfully track the motion of the microorganisms and their temperature history. In the case of vibrated flow, because of the harmonic motion of the tube wall, some of these fluid particles near the wall may move outside the numerical domain and are, therefore, ignored by the solver. In addition, some fluid particles become trapped in the slow moving fluid in the boundary layer and, thus, acquire extremely low velocities and do not reach the exit by the end of the simulation. In other words, some numerical leaking of particles is unavoidable despite using a small time-step. In order to ensure that in vibrated flow a sufficient number of fluid particles were successfully tracked

so that the flow field could be completely mapped, a large number (10^4) of such particles were introduced. The temperature and velocity histories of such particles were then used to calculate the sterility and quality profiles along the tube using a MATLAB code.

4. Validation of computational model

Though CFX is a generally well validated code as it is widely used, the computational work reported here was further validated where possible either by comparing results with theoretical solutions or literature data where possible. The intention here was to try and validate the CFD model as much as possible so as to maximise confidence in the numerical results. The various stages of the validation process are described below.

The modelling by CFD of non-Newtonian power-law fluid flow under forced vibration without heat transfer was reported and experimentally validated in our previous studies (Deshpande and Barigou, 2001; Eesa and Barigou, 2008). Comparison with experiment showed that CFD is able to predict such complex flows with a very good accuracy within approximately ±10%, under a wide range of vibration conditions. We have also reported in our recent work (Tian and Bargiou, 2015; Eesa and Barigou, 2010, 2011) detailed theoretical as well as experimental validations of temperature and heat transfer predictions from the literature in: (i) steady flow through a straight tube with wall heat transfer, of a Newtonian fluid with temperature-independent and with temperature-dependent viscosity; (ii) steady flow through a straight tube with wall heat transfer, of a non-Newtonian power-law fluid with temperature-independent viscosity.

Here, predictions of sterility and quality in a conventional continuous steady-state heat-hold-cool process are validated using an isoviscous single-phase fluid, against a simulation from Jung and Fryer (1999) executed with a different code (FIDAP). The processing conditions for this simulation are shown in Table 3. The temperature, sterility and quality profiles along the process are compared, respectively, in Figures 4 and 5, showing excellent agreement between the two simulations. Note that the volume-flowrate weighted mean temperature is calculated using Eq. (12) with T in lieu of F.

There are, however, no experimental data available on the temperature profile in flows with heat transfer when subjected to vibration. Nonetheless, given the excellent agreement of our CFD predictions of flow and heat transfer characteristics with theory and experimental results in all the above stages of the validation process, in addition to the excellent agreement of our food sterility and quality predictions to simulation results from Jung

and Fryer (1999), we believe that the present CFD model is sufficiently robust and reliable for the purposes of studying the effects of mechanical vibration on the continuous heat-hold-cool sterilisation process.

5. Results and discussion

We analyse four tube flow configurations, as shown in Figure 1: (*a*) steady flow through a straight tube as used in a conventional sterilisation process (**SF**); (*b*) steady flow through a straight tube fitted along its whole length with a Kenics static mixer (**SF-KM**); (*c*) steady flow through a straight tube with superimposed transverse oscillations (**VF**); and (*d*) steady flow through a straight tube subjected to transverse oscillations with step rotation of oscillation orientation (**VF-SR**).

5.1 Chaotic advection flow

By tracking numerous trajectories, as described in Section 3.2, we evaluated the spectrum of Lyapunov exponents which characterise the vibrated flows investigated, as defined in Section 2.3. The maximum Lyapunov exponent was found to be +0.75, which confirmed that the vibrated flows were indeed chaotic.

5.1 Effects of vibration on radial temperature distribution in heating and cooling tubes

The temperature contour plots at the exit sections of the heating and cooling tubes are displayed in Figure 6 for the four flow configurations. They demonstrate the striking improvement in radial temperature uniformity afforded by the **VF-SR** technique. The method generates a vigorous chaotic fluid motion represented by a strong vorticity field and complex spiralling fluid streamlines and trajectories (Tian and Barigou, 2015). The velocity vector distributions in Figure 6 show that, whilst in steady flow there is virtually no radial fluid motion, under vibration a secondary radial flow is superimposed on the main axial flow, which is more vigorous than that generated by the Kenics mixer. The presence of strong vortical structures is clearly apparent. This secondary chaotic advection flow, causes continuous radial mixing with hot fluid streaming from the tube wall to the centre and back in four spiralling loops, thus, generating a strong degree of radial convection which results in the quasi-uniform temperature profiles observed. Compared to simple steady flow (**SF**), over four-fold and ten-fold improvement in wall heat transfer was achieved in a heating and a cooling tube, respectively, attributed primarily to the disruption of the thermal boundary layer caused by the swirling fluid motion induced by vorticity. This radial flow increases asymptotically in strength as vibration intensifies (data not shown). Considering the heating tube, for example, the mean resultant velocity in the radial plane, $\bar{u}_{xy}$, is ~ 0 for **SF**, ~ 2.1 cm s^{-1} for **SF-**

KM, and ~ 1.1 cm s^{-1} for **VF** and **VF-SR**. Even though $\bar{u}_{xy}$ is larger for the Kenics mixer, the secondary flow is dominated by fluid body rotation which is not as effective for radial mixing as the flow generated by the wall oscillations. Similar observations apply to the cooling tube.

The axial profiles of the mean and minimum temperature are presented in Figure 7, showing rapid heating of the core region in vibrated flow. In steady laminar flow (**SF**), heat is transferred radially by conduction; therefore, in this relatively short tube (L = 2.4 m), only fluid flowing near the tube wall is significantly heated whereas the vast majority of the fluid remains at more or less the inlet temperature (Figure 6(*a*)). Heating of the inner parts of the flow is a very slow process and requires long tube lengths. The Kenics static mixer (**SF-KM**) produces much improved radial and axial temperature profiles, but results are considerably inferior to those provided by vibratory flow. In addition to its hygiene drawbacks, the Kenics mixer caused a much higher pressure drop than steady flow or flow with vibration (~ 6 – 7 folds).

Simple transverse oscillations (**VF**), however, produce four salient vortices which trap cold fluid inside and thereby hamper radial mixing and reduce temperature uniformity. By rotating the plane of oscillation in a stepwise manner (**VF-SR**), the vortex centres are made to move around, hence, causing cold fluid inside these regions to mix with hotter fluid flowing inwards from the wall, and a much improved temperature profile results radially (Figure 6(*a*)) as well as axially (Figure 7). The step rotation frequency Ω influences somewhat the wall heat transfer coefficient, the radial temperature uniformity and the mean and minimum temperatures achieved at the tube exit. The optimum value of Ω is a function of the process parameters. For example, rough numerical experiments with Ω = 0.067, 0.1, 0.2 Hz (i.e. Δt = 5, 10, 15 s), yielded the best results for 0.1 Hz giving maximum improvements of ~ 15% in wall heat transfer coefficient, ~ 200% in temperature coefficient of variation, ~ 5 °C in mean exit temperature and ~ 17 °C in minimum temperature. However, sterility and quality calculations introduce further sensitivities because of their exponential form and so, even ostensibly small differences in temperature can translate into much more significant differences in F-value and C-value. Optimum conditions can in practice be determined by adjusting the value of Ω upwards from zero until the cold vortex regions fade, a process which may require a certain amount of trial and error.

It should be noted that in this work vibration amplitude and frequency have been kept deliberately moderate (A = 2 mm, f = 50 Hz) to demonstrate that the principle works at manageable levels of vibration intensity. If higher

vibration intensities are used, these should lead asymptotically to even stronger effects. Optimum vibration conditions (amplitude and frequency) will depend on a number of factors including fluid rheology and physical properties, flowrate, tube diameter, wall and inlet temperatures. Some numerical experimentation is required to determine such conditions for a given situation. Here, we selected parameters such as fluid viscosity, temperatures, tube length, diameter etc. which represent a realistic industrial situation, but at the same time did not make the computations too costly. A detailed parametric study of the problem would require numerous and extensive simulations. Such a detailed study is beyond the scope of this paper as the main purpose here is to demonstrate the benefits of oscillatory-perturbed or chaotic advection for continuous food sterilisation.

However, whilst the value of inlet fluid viscosity used throughout the study (0.868 Pa s) is high enough to be representative of a wide range of food materials, the influence of fluid viscosity was investigated using an-order-of magnitude higher value at inlet (10 Pa s). The radial temperature and velocity vector distributions at the exit section of a heating tube corresponding to this higher inlet viscosity are presented in Figure 6(*c*) to be compared to those in Figure 6(*a*). The heat treatment in the **SF** and **SF-KM** flows is not affected by viscosity as the same degree of temperature uniformity and the same mean exit temperature are achieved in each case. As viscosity is increased from 0.868 to 10 Pa s, the mean exit temperature in the **VF** technique falls slightly by 1.3 °C, but temperature uniformity improves significantly ($C_{v\text{-}T}$ reduces from 0.0830 to 0.0500) as viscosity increases. At the same time, the mean exit temperature achieved with **VF-SR** drops significantly from 126.5 to 118.3 °C, and radial temperature uniformity deteriorates as $C_{v\text{-}T}$ increases from 0.0234 to 0.0471. However, even at 10 Pa s, **VF-SR** still outperforms the other three flow configurations, especially compared to **SF** and **SF-KM** where the margin is substantial. For this high viscosity, Ω was reduced from 0.1 to 0.08 Hz. As viscosity increases, the radial flow slows down and, to achieve better results, Ω should be reduced down to an optimum value which would enable maximum mixing of the cold vortex regions and give the best exit temperature and temperature uniformity. However, reducing Ω beyond this optimum value (e.g. in this case around 0.08 Hz for 10 Pa s) would reduce the quality of heat treatment as the benefits of the superimposed step rotation are gradually lost and **VF-SR** tends to **VF**. In this case, Ω = 0.05 Hz yielded the same results for **VF-SR** as for **VF**.

In the following sections, the benefits of the vibration techniques **VF-SR** and **VF** for a continuous heat-hold-cool sterilisation process will be compared with conventional steady-state flow (**SF**) and steady-state flow with a Kenics static mixer (**SF-KM**).

5.2 Effects of vibration on sterility in heating and cooling tubes

As discussed above, in a safe sterilisation process, all of the fluid must receive the required minimum level of lethality. In normal steady-state flow, the fluid flowing along the centreline, being the fastest, is the slowest to reach such a level of sterility. This situation is much worse for viscous fluids flowing in the laminar regime. The challenge facing any continuous process of this kind, therefore, is to ensure that the fluid at the centre is safe without overcooking too much the slow-moving fluid near the hot tube wall.

5.2.1 Heating stage

Using the massless particle tracking algorithm described above, the temperature history profiles obtained by CFD in a heating tube were used to compute the radial sterility distribution at different axial positions. As pointed out above, in these calculations the thin boundary layer region (1 mm) adjacent to the hot wall was ignored, as it contains extremely large F-values (in this region $F \rightarrow \infty$). Radial contour plots of sterility at the exit section of the heating tube are shown in Figure 8 together with plots of azimuthally-averaged F-values. The **VF-SR** technique produces the highest local F-values. Results for steady flow show that $F \ll 10^{-2}$ over about 80% of the tube radius, and increases exponentially towards the wall reaching extremely high values, many orders of magnitude greater than the value at the centre (hence the use of a log scale). In contrast, due to better radial mixing, steep variations in F are confined within a much narrower (~ 1 mm) annular wall region for the other three flow regimes, thus reducing the impact of the wall region on the heat treatment of the fluid.

As shown in Table 4, the volume-flowrate weighted mean sterility $\bar{F}_{\boldsymbol{VF-SR}}$ is much greater than for the other flow regimes ($117.5 \times \bar{F}_{\boldsymbol{SF}}$; $21.7 \times \bar{F}_{\boldsymbol{SF-KM}}$; $5.3 \times \bar{F}_{\boldsymbol{VF}}$). The uniformity of the radial F distribution across the tube section is also the best ($C_{v\text{-}F}$ ~ 1.09), significantly better than for **VF** ($C_{v\text{-}F}$ ~ 1.33) and substantially better than for **SF-KM** ($C_{v\text{-}F}$ ~ 1.58) and **SF** ($C_{v\text{-}F}$ ~ 3.75). As a result of the remarkable radial uniformity of the F-value achieved by **VF-SR**, the mean value $\bar{F}$ across the tube, is very similar to the local F-values; in particular the ratio of $\bar{F}$ to F_c, the value at the centre, which conventionally in steady flow is regarded as the coldest point, is ~ 1.0 – note because of its chaotic nature, in vibrated flow the coldest point is not located at the centre. In steady flow, however, $\bar{F} \sim 8{\times}10^{7} \times F_c$. The static mixer shows segregation areas of very low F-values, and the four cold vortex regions are also apparent in the **VF** contours as regions of low sterility (Figure 8), but the latter regime still outperforms the **SF-KM** configuration, yielding a mean F-value which is several times higher.

The values of the minimum sterility achieved, F_{min}, are also shown in Table 4. These values are in the main much smaller than $\bar{F}$, and the relative superiority of **VF-SR** over the other configurations (**SF**, **SF-KM**, **VF**) based on minimum sterility is even more staggering (respectively, ~ 3.2×10^9, ~ 146 and ~ 94 folds).

The above results also serve to show the potential danger of using $\bar{T}$ and $\bar{F}$ to assess the thermal processing of the fluid. As the fluid flows in parallel layers which do not mix, $\bar{F}$ is clearly not a reliable measure of sterility in steady flow, so that high mean values do not necessarily imply a safe level of sterility. Even with the Kenics mixer the temperature history along the tube results in many scattered pockets where the local F-value is ~ 20 times smaller than $\bar{F}$. The use of an average F-value may only be justifiable in a radially well-mixed flow such as the vibrated flow (**VF-SR**) considered here, where chaotic advection ensures that fluid elements continuously exchange radial position along the tube, thus, narrowing the residence time distribution as well as the radial temperature distribution. Consequently, a more rational evaluation of these different thermal processing regimes should be based on the minimum local sterility value, F_{min}, achieved at exit.

There is also a marked difference in the axial growth of F_{min} between the four types of flow, as shown in Figure 9. In steady flow and in steady flow with the Kenics mixer, F_{min} rises very slowly along the tube. On the other hand, under vibration, radial mixing ensures that the fluid at the tube centre is heated much more rapidly, thus causing F_{min} to grow rapidly with z; the effect is much more pronounced for **VF-SR** than for **VF**, however (Figure 9). It follows, therefore, that with chaotic advection a given level of sterility can be achieved in much shorter tubes. For example, for the process conditions considered here, achieving the minimum sterility value of 12.5 s obtained with **VF-SR** in the 2.4 m long tube, as shown in Figure 10, would require a heater which has a length of ~ 26.0 m with **SF**, ~ 4.0 m with **SF-KM** and ~ 3.2 m with **VF**. To stress the point made above about the danger of using mean sterility as a guide, comparison on the basis of $\bar{F}$ would suggest instead that the **SF** tube should only be ~ 7.7 m long.

5.2.2 Cooling stage

In the cooling stage of a heat-hold-cool process, to preserve as much of the product quality as possible, ideally the cooking process should not proceed any further. Thus, further build-up of sterility along the tube is undesirable. The mean values of sterility reached at the end of a cooling tube operating under the four different flow regimes are given in Table 4, whilst the variations of $\bar{F}$ along the tube are plotted in Figure 11 alongside

radial contour plots and azimuthally-averaged profiles of sterility. For discussion purposes and to enable easy comparison of the performance of the four different flow configurations, in this case the same uniform temperature of 126.6 °C was used at the inlet of each cooling tube. This, in fact, is the temperature reached at the exit of the **VF-SR** heating tube. Note that the sterility values obtained in the cooling tubes of **SF**, **SF-KM** and **VF** are higher than those obtained in their corresponding heating tubes, but only because the high inlet temperature (126.6 °C) assumed for these three flow regimes would in practice require much longer ($\gg$ 2.4 m) heating tubes to achieve it, in which case the sterility accumulated in the heater would also be correspondingly much higher than in the cooler.

Under **SF**, there is a substantial monotonic growth in $\bar{F}$ with z. The **SF-KM** configuration causes initially a considerable rise in F, reaching a plateau after ~ 1.0 m. With vibration superimposed on the flow, for both **VF** and **VF-SR** there is an initial rise in the F-value over a short length of tube, levelling off at a ~ 0.6 m and reaching about 60% of the $\bar{F}$ value attained with **SF-KM**. Thus, vibrated flow is by far the closest to the ideal situation of zero cooking in a cooling tube. Furthermore, similar to the heating tube, vibration has the added advantage of producing nearly uniform distributions of F across the cooling tube cross-section, as shown in Figure 11; the corresponding $C_{v\text{-}F}$ values are given in Table 4.

The four salient vortex regions observed in the **VF** heating tube (see Figure 8) are still apparent in Figure 11; these are detrimental to mixing and prevent effective fluid cooling. As a result, these vortex regions are now regions of relatively high sterility contrary to the situation in the heating tube.

5.3 Effects of vibration on quality in heating and cooling tubes

5.3.1 Heating stage

For a given amount of heat treatment, i.e. for a given sterility value F, the quality value C, defined above in Eq. (10) should be as low as possible. Contours of the radial distribution of quality as well as the azimuthally-averaged radial profiles for the four flow regimes studied are compared in Figure 12, for a given minimum sterility F_{min} = 12.5 s, which is the value achieved at the exit of the 2.4 m **VF-SR** tube. As discussed above, and as shown in Figure 10, to achieve this same sterility value, **SF** requires ~ 26.0 m of heating tube, **SF-KM** requires ~ 4.0 m and **VF** requires ~ 3.2 m. Clearly, **VF-SR** produces the lowest and most uniform C-values ($C_{v\text{-}C}$ values are given in Table 5), outperforming by far the traditional steady flow process as well as the Kenics mixer.

5.3.2 Cooling stage

As discussed above, vibrating the flow in the heating tube led to a fast rise in fluid temperature along the tube (Figure 7). Similarly, vibration causes a fast drop in fluid temperature in the cooling tube which helps to minimize the loss of product quality. The variations of $\bar{C}$ along the tube, depicted in Figure 13, show how vibration quickly limits the rise in quality value. Both **VF** and **VF-SR** achieve a low plateau after a short length of tubing, whilst **SF-KM** shows a substantial rise in C-value about twice as high. In contrast, **SF** exhibits a large monotonic increase in $\bar{C}$ as a function of *z*. The radial quality contours at the exit are also shown in Figure 13, whilst the corresponding $C_{v\text{-}C}$ values are given in Table 4. Again, the **VF-SR** regime gives the best uniformity in quality distribution across the cooling tube. The Kenics mixer (**SF-KM**) performs considerably better than **SF** both in terms of mean quality and uniformity achieved, but it is much inferior to **VF** and **VF-SR**.

5.4 The heat-hold-cool process

In this section, we assess the complete heat-hold-cool process under the four different flow regimes studied using the simulation parameters shown in Table 6. The mean temperature history curves for these four processes are compared in Figure 14. The **VF-SR** process comes on top achieving fast heating and fast cooling, outperforming by a substantial margin the conventional steady-state process both with and without the Kenics static mixer. In terms of temperature profile, simple transverse vibration (**VF**) compares reasonably well with **VF-SR**, but, as pointed out earlier, the seemingly modest differences in temperature in fact translate into large (an order of magnitude) differences in minimum sterility in favour of **VF-SR**, as shown in Figure 15. The **VF-SR** heat-hold-cool process achieves $F_{min} = 190.9$ s at the end of the holding stage with minimal increase in sterility during cooling. As shown in Figure 15, this same value can be achieved in a heating tube which is only slightly longer (~ 0.43 m) but with less quality loss than when a **VF-SR** holding tube (2.4 m) is used ($\bar{C} = 48.5$ s compared to 104.1 s).

To achieve a given level of sterility, the question then arises as to whether it would be better to use a vibrated holding tube, or instead use an extended vibrated heating tube and conduct all the sterilisation within the heating stage? The overall performance of an extended **VF-SR** heater is compared with that of a **VF-SR** holding tube in Figure 16, where the increase ΔF_{min} and the associated increase $\Delta\bar{C}$ for both tubes are plotted as a function of *z*. The results demonstrate that there are considerable benefits in using an extended heater and, perhaps for most applications, a holding stage may not be necessary if a **VF-SR** heating stage is used. The use of a vibrated heater

would then seem to obviate the need for a holding tube which represents an additional significant advantage. However, if a holding stage is used, even though the radial temperature profile at the exit of the vibrated heater would usually be virtually uniform, it appears that there would still be some significant advantage in vibrating the holding tube. Results in this case showed that, whilst the mean sterility achieved would be the same, vibrating the holding tube (2.4 m) would yield a minimum sterility which is ~ 65% greater (equivalent to using a 4.0 m non-vibrated holding tube).

The axial profiles of mean quality along the whole process depicted in Figure 17 considered together with the sterility profiles in Figure 15 show that for an-order-of-magnitude larger minimum sterility, **VF-SR** incurs an average quality loss comparable to that of **VF** in a process of the same length. Similarly, for about 2 to 10 orders of magnitude difference in minimum sterility between **VF-SR**, **SF-KM and SF**, the **VF-SR** process incurs an average quality loss only about an order of magnitude greater. Results in Figures 10 and 12 have also shown how **VF-SR** severely limits the rise in F and C in the cooling stage. Combined together, these results indicate that **SF**, **SF-KM** and **VF** processes which would produce equivalent sterility to the **VF-SR** process would have to be extremely long by comparison and would generate orders of magnitude more quality loss. Hence, the whole sterilisation process can be performed using only two relatively short heat-cool processing tubes.

6. Conclusions

The superimposition of transverse vibratory motion with step change in oscillation orientation on the steady laminar flow of a viscous single-phase fluid, introduces chaotic fluid motion which leads to significant improvements in wall heat transfer and radial temperature uniformity. When applied to a continuous heat-hold-cool sterilisation process, these effects translate into much better thermal processing uniformity and product quality compared with a conventional process with or without an inline static mixer fitted. Simple oscillations without a change in orientation also give good improvements but they are not nearly as effective.

The novel (**VF-SR**) technique leads to faster nearly-uniform heating and cooling of the product, thus, achieving substantially higher levels of sterility with low loss of product quality in much shorter processing tubes, thus, obviating the need for a holding stage and overall reducing the length of the conventional heat-hold-cool sterilisation process by one or two orders of magnitude, depending on processing conditions. Vibration, therefore, appears to create processing conditions that are much more in agreement with the high temperature for

short time (HTST) assumption which is often contradicted in conventional steady flow processing. This shows that the **VF-SR** technique has considerable potential in optimising the continuous sterilisation process by creating conditions for achieving HTST processing, a long-standing problem in food sterilisation.

Whilst this numerical analysis has been well validated, a full experimental validation, as is usual industrial practice, would be needed to fully confirm the benefits of oscillatory perturbations on the microbial sterilisation process. It should also be noted that the above conclusions are only valid for single-phase flows as considered in this analysis. Heat transfer in two-phase solid-liquid flows where particle properties such as size and density are such that the mixture cannot be treated as a homogenous fluid, is much more complex and the applicability of the oscillatory perturbation technique to such flows warrants a more detailed study.

Furthermore, it can be argued that the chaotic flow would have added practical benefits: first, for the reduction of fouling because of the cleaning action that the fluid motion would create at the wall, and second in two-phase solid-liquid flow, assuming that the applicability of the oscillatory technique is proven, it would be expected to help keep solid particles in suspension and may also potentially enhance liquid-particle heat transfer. The implementation of mechanical vibration in practice should not be difficult. To avoid mechanical fatigue, the vibrated pipe should be connected to other pipework via flexible piping or flexible couplings. Whilst the use of vibration industrially may not always be feasible, in processes where this is possible, however, results indicate that benefits can be significant.

Acknowledgements

Shuai Tian's PhD research was funded by a China Government & University of Birmingham scholarship.

Notation

A Vibration amplitude, m

C Quality value, s

$\bar{C}$ Volume-flowrate weighted mean quality value, s

C_p Specific heat capacity, J kg^{-1} K^{-1}

$C_{v\text{-}C}$ Coefficient of variation for quality value, (-)

$C_{v\text{-}F}$ Coefficient of variation for sterility value, (-)

$C_{v\text{-}T}$ Coefficient of variation for temperature, (-)

E_a Activation energy for viscosity, J mol^{-1}

F Sterility value, s

F_{min} Minimum sterility value at given cross–section, s

$\bar{F}$ Volume-flowrate weighted mean sterility value, s

f Vibration frequency, Hz

k_0 Pre-exponential factor, Pa s

L Tube length, m

r Radial position, m

R Radius of tube, m

R_g Gas constant, J mol^{-1} K^{-1}

t Time, s

Δt Time interval, s

T Temperature, °C

$\bar{T}$ Volume-flowrate weighted mean temperature, °C

T_{in} Inlet temperature, °C

$\bar{T}_{out}$ Volume-flowrate averaged temperature at the tube exit, °C

T_w Wall temperature, °C

u Velocity in radial direction, m s^{-1}

$\bar{u}_{xy}$ Mean resultant velocity in radial plane, m s^{-1}

$\overline{w}$ Mean inlet velocity, m s^{-1}

w Velocity in axial direction, m s^{-1}

x Wall displacement, m

z Axial position, m

Greek symbols

μ Viscosity for Newtonian fluid, Pa s

ρ Density, kg m^{-3}

λ Thermal conductivity, W m^{-1} K^{-1}

ω Angular function of frequency of vibration, rad s^{-1}

Ω Frequency of step rotation of oscillation orientation, Hz

References

Barigou M., Mankad S., Fryer P.J., 1998. Heat transfer in two-phase solid-liquid food flows: A review. Food Bioprod. Process. 76, 3-29.

Barth, T.J., Jesperson D.C., 1989. The design and application of upwind schemes on unstructured meshes. AIAA, pp. 1-12 [AIAA, paper 89-0366].

Bird R.B., Armstrong R.C., Hassager O., Curtiss C.F., 1987. Dynamics of Polymeric Liquids: Fluid Mechanics, second Ed Vol. 1. John Wiley, New York.

Chagny C., Castelain C., Peerhossaini H., 2000. Chaotic heat transfer for heat exchanger design and comparison with a regular regime for a large range of Reynolds numbers. Appl. Therm. Eng. 20, 1615-1648.

David J.R.D., Graves R.H., Szemplenski T., 2012. Handbook of Aseptic Processing and Packaging, second Ed. Taylor & Francis, London.

Deshpande N.S., Barigou M., 2001. Vibrational flow of non-Newtonian fluids. Chem. Eng. Sci. 56, 3845-3853.

Eesa M., Barigou M., 2008. CFD analysis of viscous non-Newtonian flow under the influence of a superimposed rotational vibration. Comput. Fluids 37, 24-34.

Eesa, M., Barigou, M., 2010. Enhancing radial temperature uniformity and boundary layer development in viscous Newtonian and non-Newtonian flow by transverse oscillations: A CFD study. Chemical Engineering Science. 65(6), 2199-2212.

Eesa, M., Barigou, M., 2011. CFD simulation of transverse vibration effects on radial temperature profile and thermal entrance length in laminar flow. AIChE Journal. 57(1), 51-56.

Godfrey J.C., 2000. Static mixers, in "Mixing in the process industries", ed. N. Harnby, M.F. Edwards, A.W. Nienow, Ch. 12, pp.225-249. 2nd Edition, Butterworth-Heinemann, Oxford.

Gundogdu M.Y., Carpinlioglu M.O., 1999. Present state of art on pulsatile flow theory – (Part 1: Laminar and transitional flow regimes). JSME Int. J. Ser. B.–Fluids Therm. Eng. 42, 384-397.

Hobbs D.M., Muzzio F.J., 1997. The Kenics static mixer: a three-dimensional chaotic flow. Chem. Eng. J. 67, 153-166.

Holdsworth S.D., 1992. Aseptic processing and packaging of food products. Elsevier Applied Science, London.

Jakobsen H.A., 2014. Chemical Reactor modelling: Multiphase reactive flows. 2nd Edition, Springer.

Jung A., Fryer P.J., 1999. Optimising the quality of safe food: Computational modelling of a continuous sterilisation process. Chem. Eng. Sci. 54, 717-730.

Kantz, H., Schreiber, T.U., 2004. Nonlinear time series analysis. Cambridge University Press.

Mostofa M.G., Kil K., Hwan A., 2010. Computational fluid analysis of abrasive waterjet cutting head. J. Mech. Sci. Tech. 24, 249-252.

Saatdjian E., Rodrigo A.J.S., Mota J.P.B., 2012a. On chaotic advection in a static mixer. Chem. Eng. J. 187, 289-298.

Saatdjian E., Rodrigo A.J.S., Mota P.B., 2012b. A study of mixing by chaotic advection in two three-dimensional open flows. Chem. Eng. Sci. 81, 179–190.

Shrirao P.N., Sambhe R.U., Bodade P.R., 2013. Convective heat transfer analysis in a circular tube with different types of internal threads of constant pitch. Int. J. Eng. Adv. Tech. 2, 335-340.

Steffe J.F., 1996. Rheological Methods in Food Process Engineering, second Ed. Freeman Press, East Lansing, Michigan.

Tian S., Barigou M., 2015. An improved vibration technique for enhancing temperature uniformity and heat transfer in viscous fluid flow. Chem. Eng. Sci. 123, 609-619.

Figure and Table Captions

Figure 1. Flow configurations: (*a*) steady flow through a tube (**SF**); (*b*) steady flow through a tube fitted with a Kenics static mixer (**SF-KM**), showing 4 elements out of 48; (*c*) flow through a tube subjected to transverse oscillations (**VF**); (*d*) flow through a tube subjected to transverse oscillations with step rotation of vibration orientation (**VF-SR**).

Figure 2: Illustration of grid used on MATLAB for evaluation of volume-flowrate weighted mean temperature, sterility and quality over tube cross-section (total number of cells, N = 1860 cells).

Figure 3. Computational mesh: (*a*) **SF**, **VF** and **VF-SR**; (*b*) **SF-KM**.

Figure 4. Validation of CFD-predicted temperature profiles in a heat-hold-cool process against simulation results from Jung & Fryer (1999) for the processing conditions of Table 3.

Figure 5. Validation of CFD-predicted sterility and quality profiles in a heat-hold-cool process against simulation results from Jung & Fryer (1999) for the processing conditions of Table 3.

Figure 6. Radial temperature and velocity vector distributions at the exit sections of processing tubes of the same length (L = 2400 mm): (*a*) heating tube ($k_0 = 5.0 \times 10^{-7}$ Pa s; T_{in} = 20 °C; T_w = 140 °C; Ω = 0.1 Hz); (*b*) cooling tube ($k_0 = 5.0 \times 10^{-7}$ Pa s; T_{in} = 126.5 °C; T_w = 20 °C; Ω = 0.1 Hz); and (*c*) heating tube with 10 Pa s inlet viscosity compared to 0.868 Pa s in (*a*) ($k_0 = 5.75 \times 10^{-6}$ Pa s; T_{in} = 20 °C; T_w = 140 °C; Ω = 0.08 Hz).

Figure 7. Development of mean and minimum temperature along heating tubes of the same length: T_{in} = 20 °C; T_w = 140 °C; L = 2400 mm.

Figure 8. Azimuthally-averaged radial profiles and contour plots of F-value at the exit section of heating tubes of the same length: T_{in} = 20 °C; T_w = 140 °C; L = 2400 mm.

Figure 9. Development of minimum F-value along heating tubes of the same length: T_{in} = 20 °C; T_w = 140 °C; L = 2400 mm.

Figure 10. Development of minimum F-value along heating tubes of different lengths with different flow regimes achieving the same value (F_{min} = 12.5 s) at the exit section: T_{in} = 20 °C; T_w = 140 °C.

Figure 11. Development of mean F-value in cooling tubes of the same length: showing axial profile of mean sterility, contour plots and azimuthally-averaged radial profiles of F-value at the exit section: T_{in} = 126.5 °C; T_w = 20 °C; L = 2400 mm.

Figure 12. Azimuthally-averaged radial profiles and contour plots of C-value at the exit section of heating tubes of different lengths with different flow regimes achieving the same mean sterility (F_{min} = 12.5 s) at the exit section: T_{in} = 20 °C; T_w = 140 °C (note the red colour in the **SF** contour exceeds the top of the scale by 2 orders of magnitude).

Figure 13. Development of mean C-value in cooling tubes of the same length: showing axial profile of mean quality and contour plots of C-value at the exit section: T_{in} = 126.5 °C; T_w = 20 °C; L = 2400 mm.

Figure 14. Development of mean temperature along heat-hold-cool process: T_w = 140 °C (heating); T_w = 20 °C (cooling)

Figure 15. Development of minimum F-value along heat-hold-cool process: T_w = 140 °C (heating); T_w = 20 °C (cooling) – process axial temperature profile shown in Figure 14.

Figure 16. Increase in minimum sterility and mean quality arising from extending the **VF-SR** heating tube compared with using a **VF-SR** holding tube.

Figure 17. Development of mean C-value along heat-hold-cool process: T_w = 140 °C (heating); T_w = 20 °C (cooling) – process axial temperature profile shown in Figure 14

Table 1: Rheological parameters used in simulations.

Table 2: Dimensions of Kenics static mixer (Figure 1(*b*)).

Table 3: Process parameters (Jung and Fryer, 1999).

Table 4: Mean sterility and quality in heating and cooling stages.

Table 5: Mean exit quality in heating tubes achieving the same minimum sterility at exit (F_{min} = 12.5 s).

Table 6: Simulation parameters for complete heat-hold-cool process.

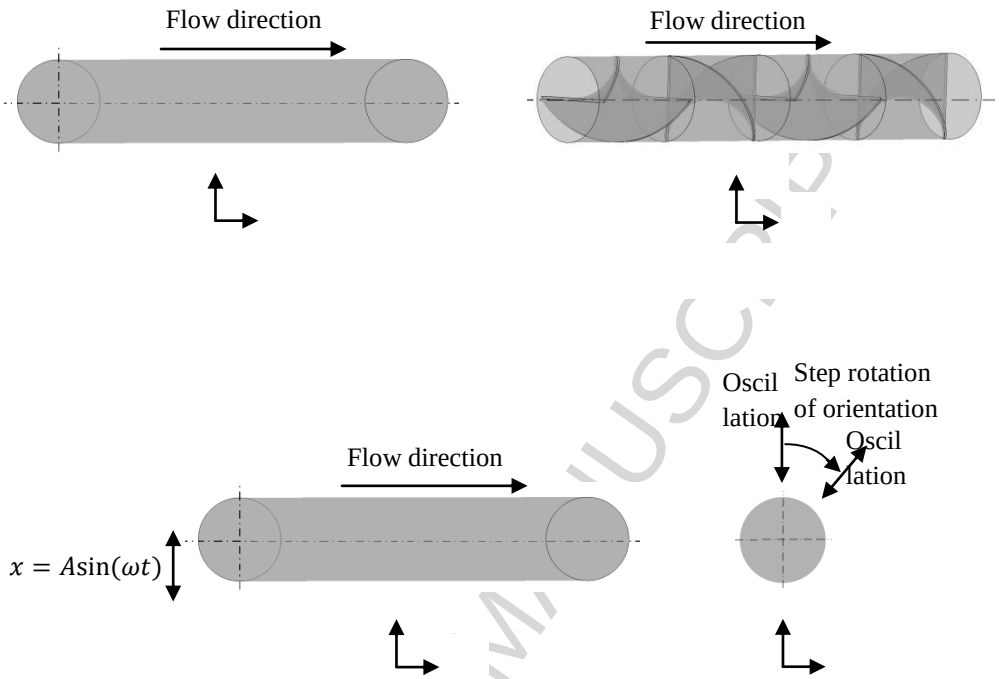

Figure 1. Flow configurations: (*a*) steady flow through a tube (**SF**); (*b*) steady flow through a tube fitted with a Kenics static mixer (**SF-KM**), showing 4 elements out of 48; (*c*) flow through a tube subjected to transverse oscillations (**VF**); (*d*) flow through a tube subjected to transverse oscillations with step rotation of vibration orientation (**VF-SR**).

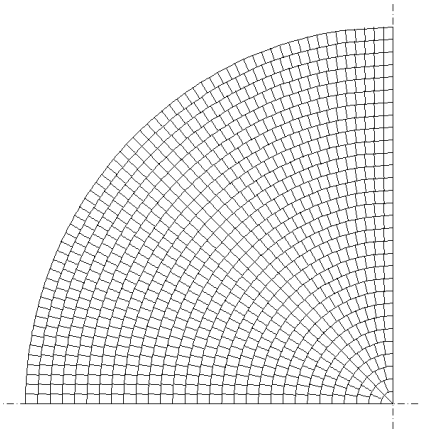

Figure 2: Illustration of grid used on MATLAB for evaluation of volume-flowrate weighted mean temperature, sterility and quality over tube cross-section (total number of cells, N = 1860 cells).

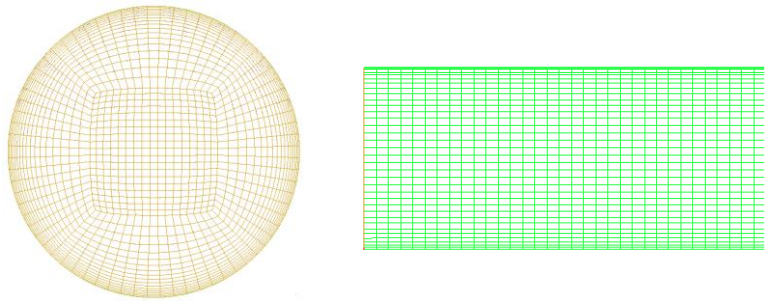

(a) SF, VF, VF-SR

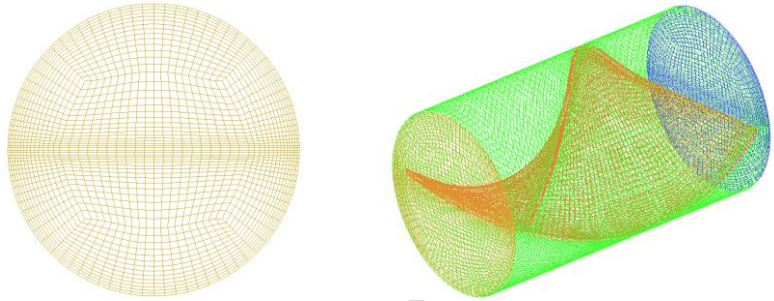

(b) SF-KM

Figure 3. Computational mesh: (*a*) **SF**, **VF** and **VF-SR**; (*b*) **SF-KM**.

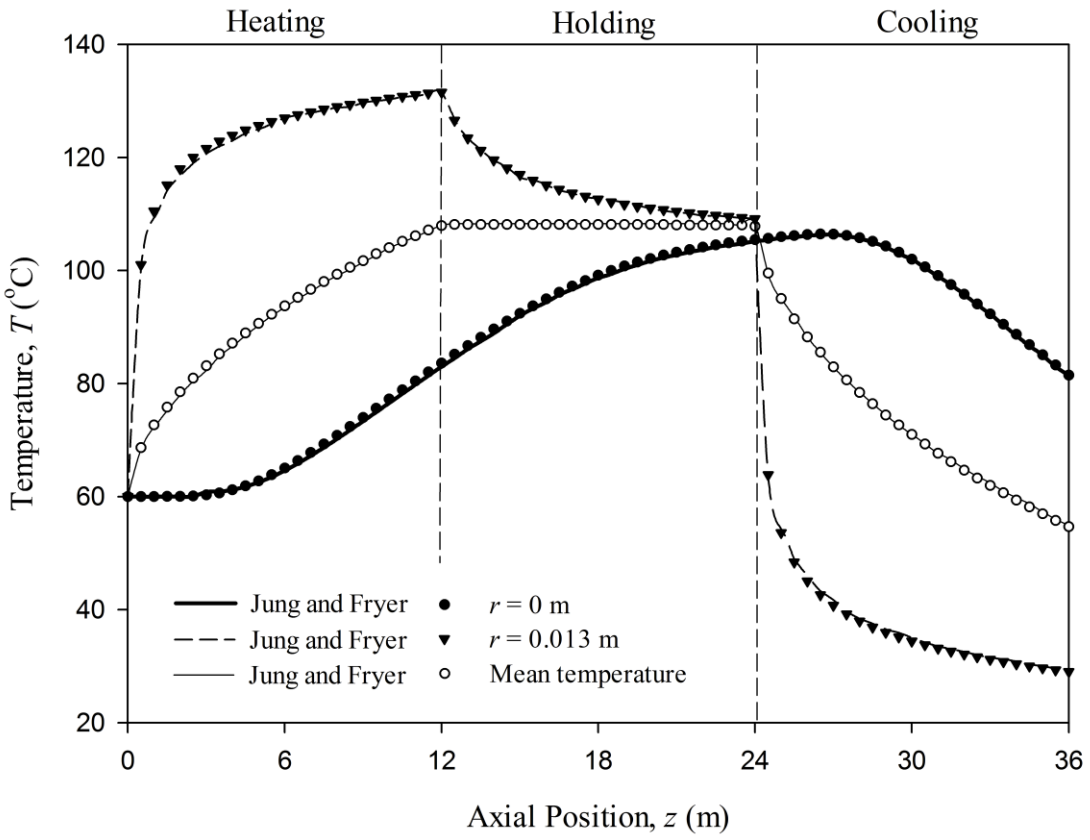

Figure 4. Validation of CFD-predicted temperature profiles in a heat-hold-cool process against simulation results from Jung & Fryer (1999) for the processing conditions of Table 3.

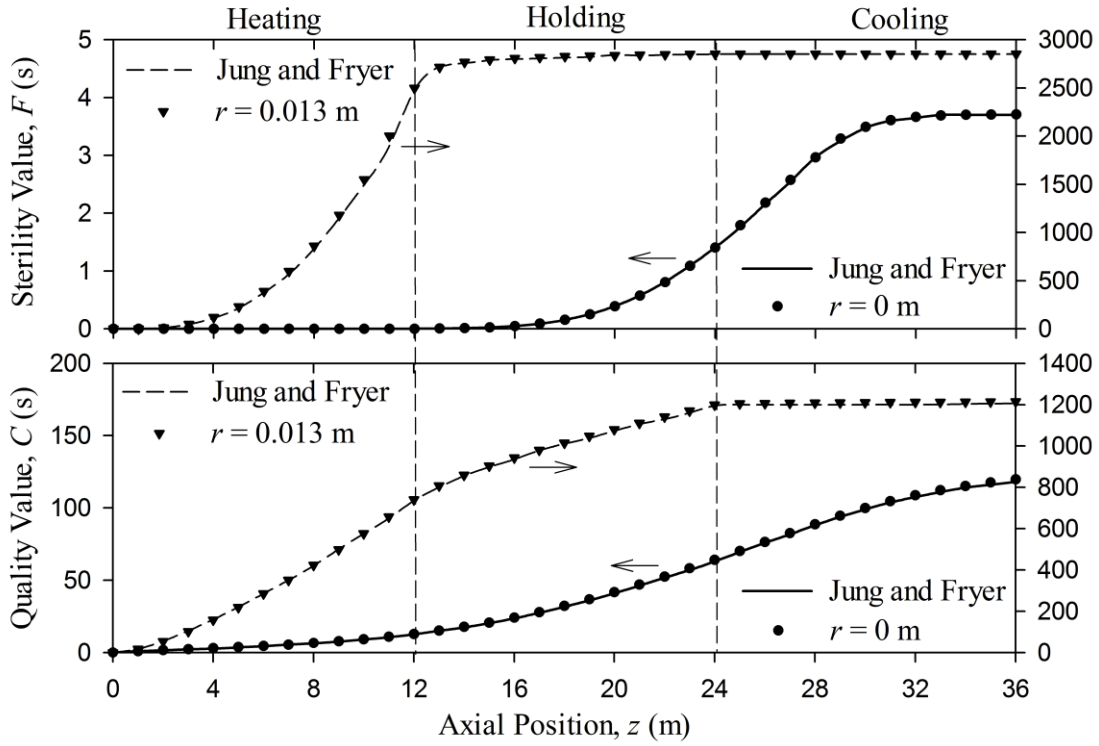

Figure 5. Validation of CFD-predicted sterility and quality profiles in a heat-hold-cool process against simulation results from Jung & Fryer (1999) for the processing conditions of Table 3.

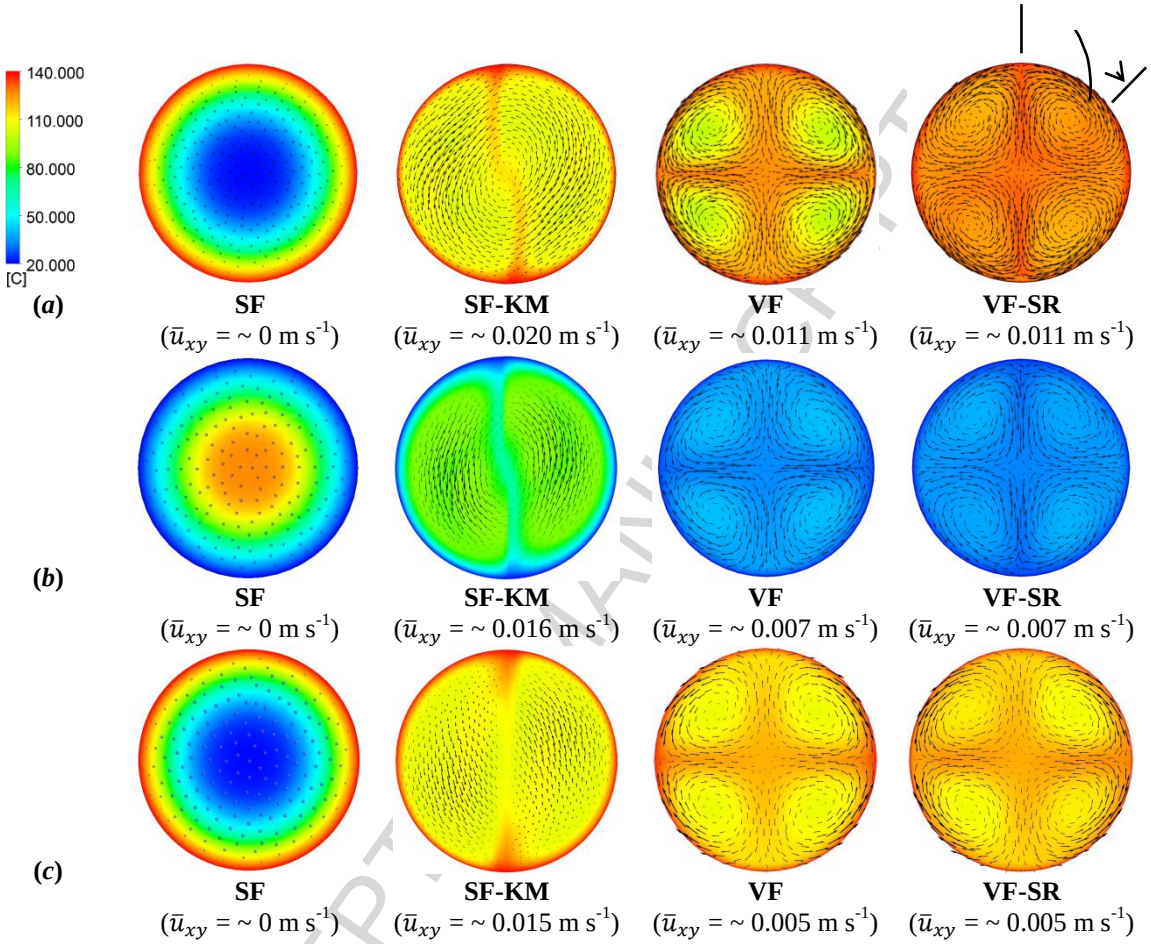

Figure 6. Radial temperature and velocity vector distributions at the exit sections of processing tubes of the same length (L = 2400 mm): (*a*) heating tube (k_0 = 5.0 × 10^{-7} Pa s; T_{in} = 20 °C; T_w = 140 °C; Ω = 0.1 Hz); (*b*) cooling tube (k_0 = 5.0 × 10^{-7} Pa s; T_{in} = 126.5 °C; T_w = 20 °C; Ω = 0.1 Hz); and (*c*) heating tube with 10 Pa s inlet viscosity compared to 0.868 Pa s in (*a*) (k_0 = 5.75 × 10^{-6} Pa s; T_{in} = 20 °C; T_w = 140 °C; Ω = 0.08 Hz).

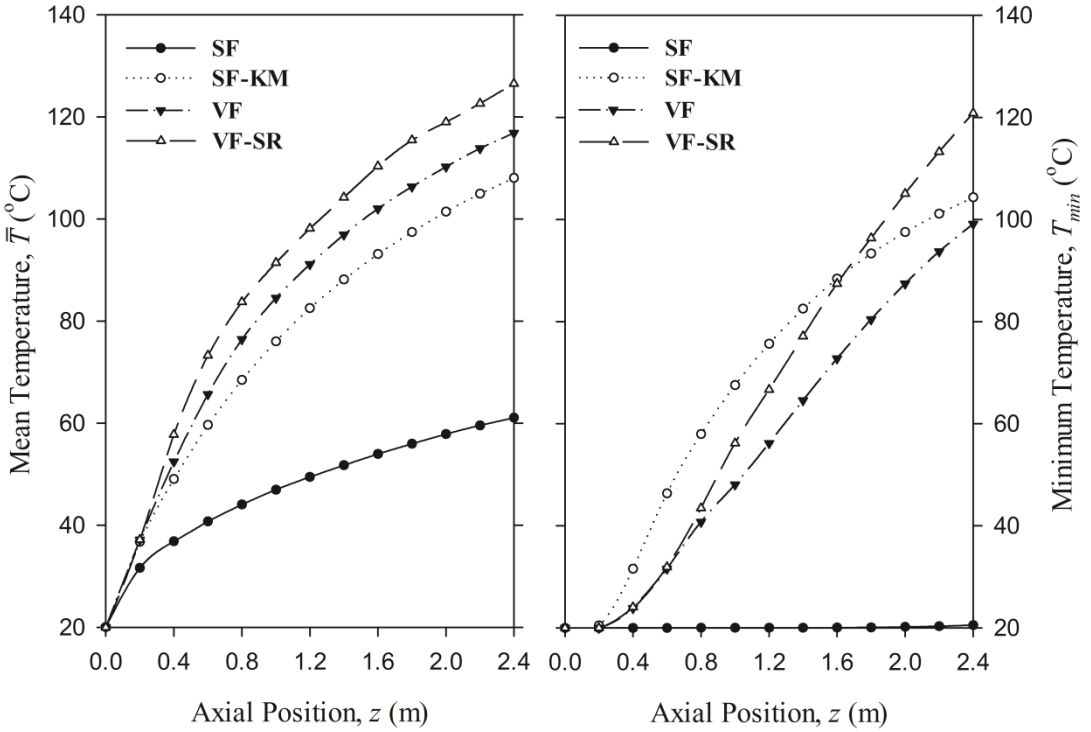

Figure 7. Development of mean and minimum temperature along heating tubes of the same length: T_{in} = 20 °C; T_w = 140 °C; L = 2400 mm.

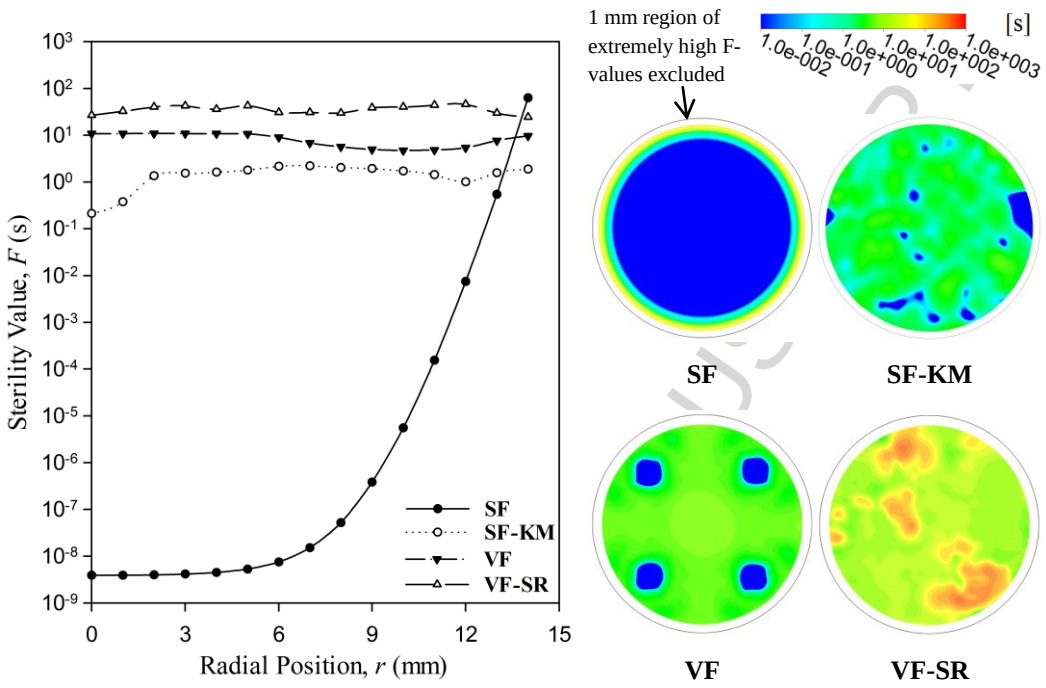

Figure 8. Azimuthally-averaged radial profiles and contour plots of F-value at the exit section of heating tubes of the same length: T_{in} = 20 °C; T_w = 140 °C; L = 2400 mm.

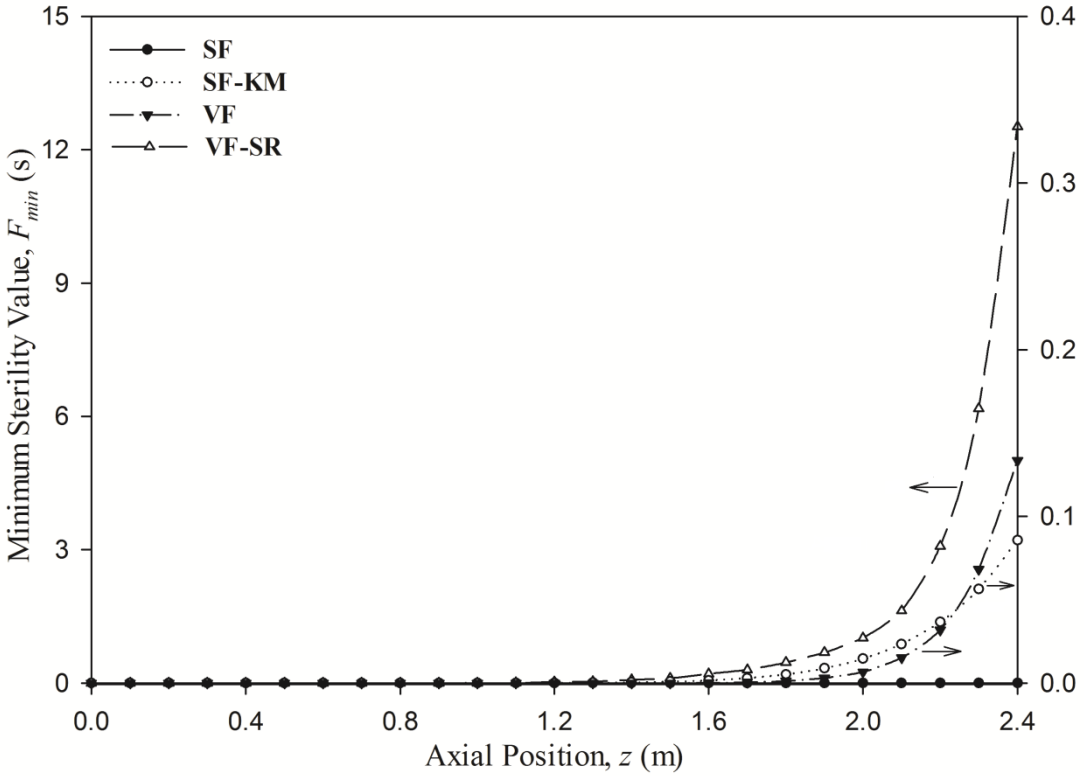

Figure 9. Development of minimum F-value along heating tubes of the same length: T_{in} = 20 °C; T_w = 140 °C; L = 2400 mm.

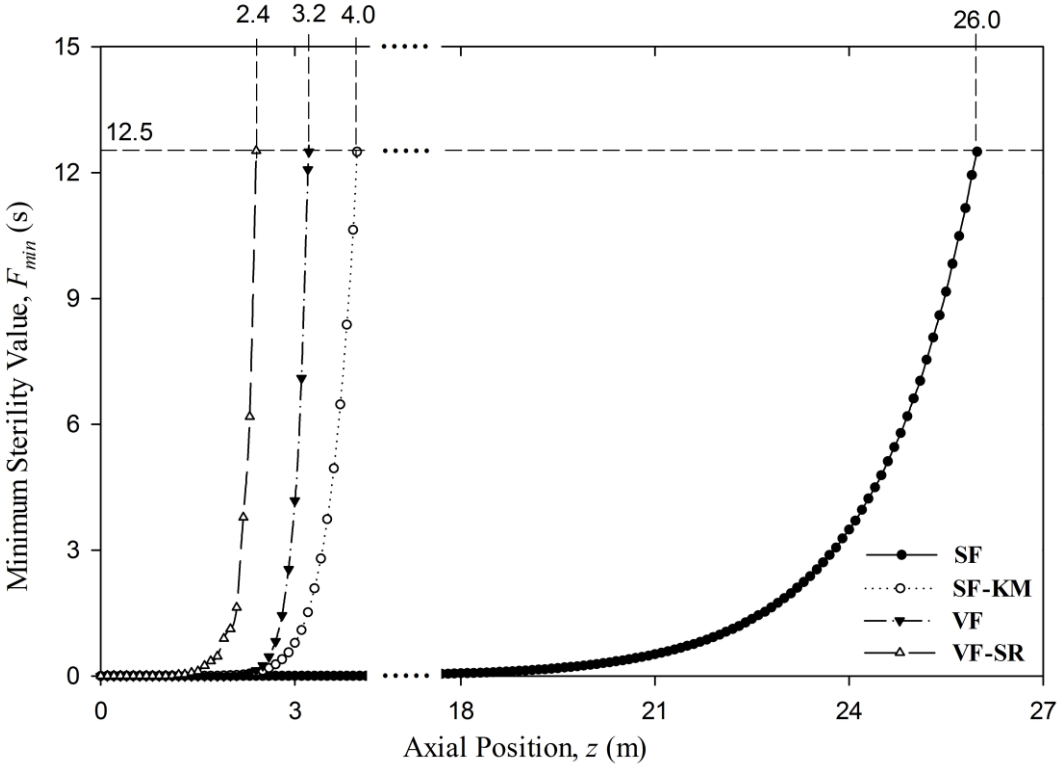

Figure 10. Development of minimum F-value along heating tubes of different lengths with different flow regimes achieving the same value (F_{min} = 12.5 s) at the exit section: T_{in} = 20 °C; T_w = 140 °C.

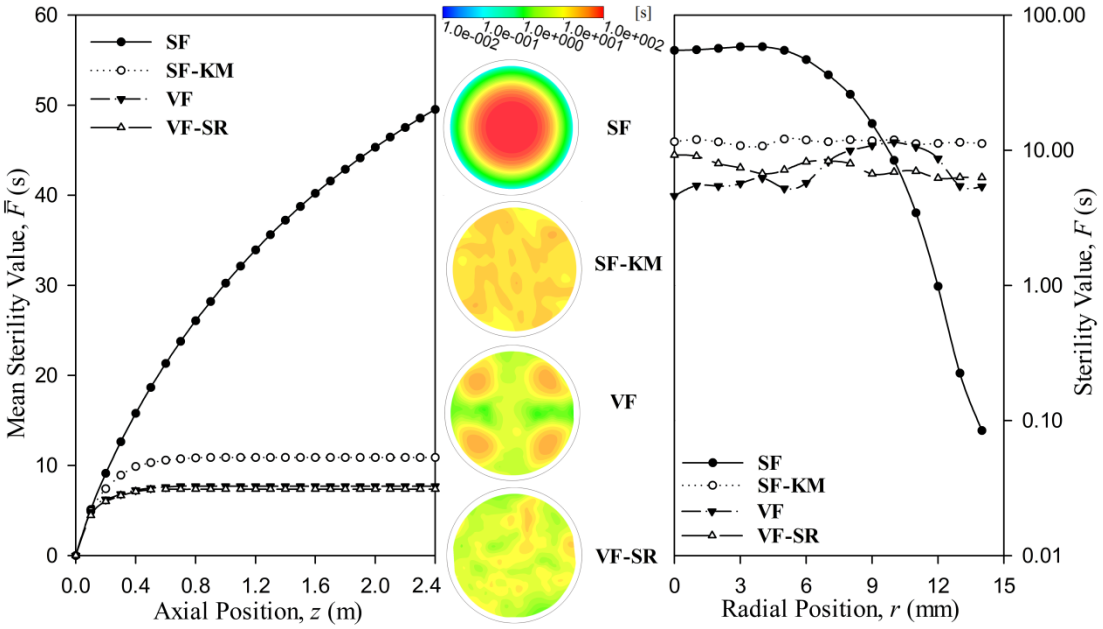

Figure 11. Development of mean F-value in cooling tubes of the same length: showing axial profile of mean sterility, contour plots and azimuthally-averaged radial profiles of F-value at the exit section: T_{in} = 126.5 °C; T_w = 20 °C; L = 2400 mm.

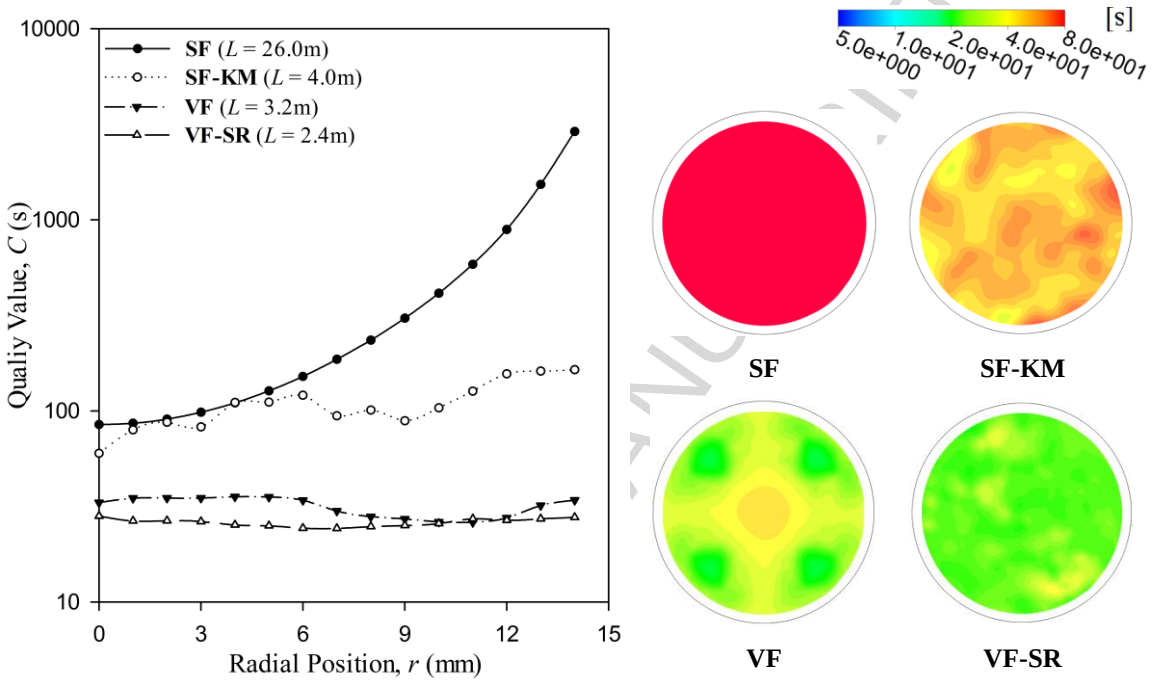

Figure 12. Azimuthally-averaged radial profiles and contour plots of C-value at the exit section of heating tubes of different lengths with different flow regimes achieving the same mean sterility (F_{min} = 12.5 s) at the exit section: T_{in} = 20 °C; T_w = 140 °C (note the red colour in the **SF** contour exceeds the top of the scale by 2 orders of magnitude).

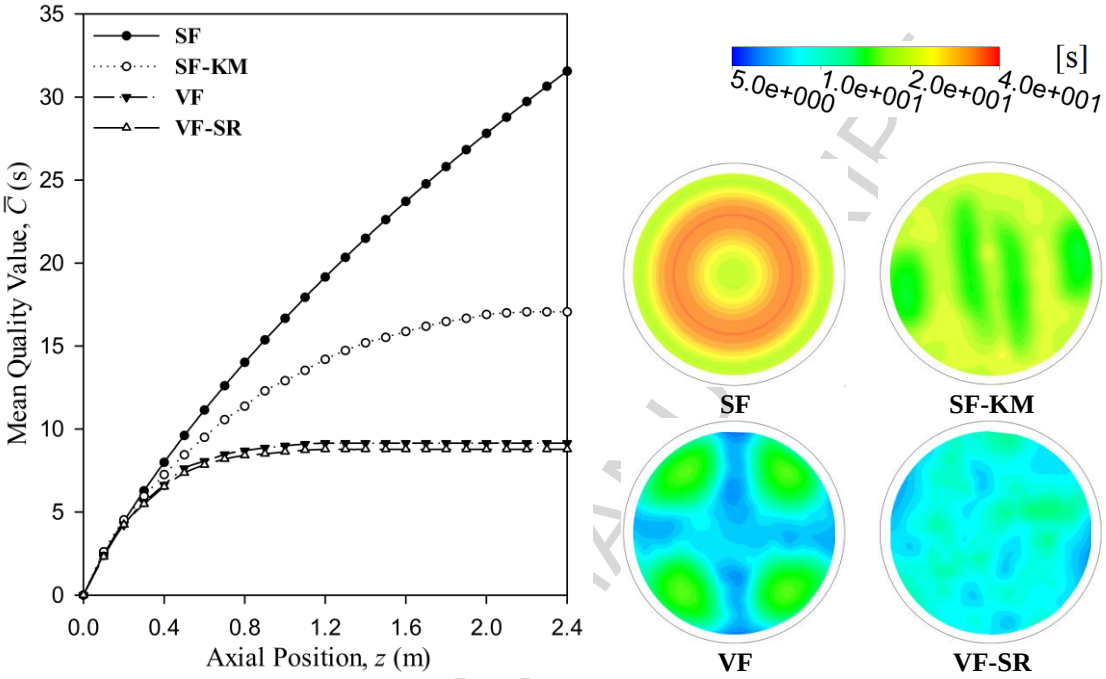

Figure 13. Development of mean *C*-value in cooling tubes of the same length: showing axial profile of mean quality and contour plots of C-value at the exit section: T_{in} = 126.5 °C; T_w = 20 °C; L = 2400 mm.

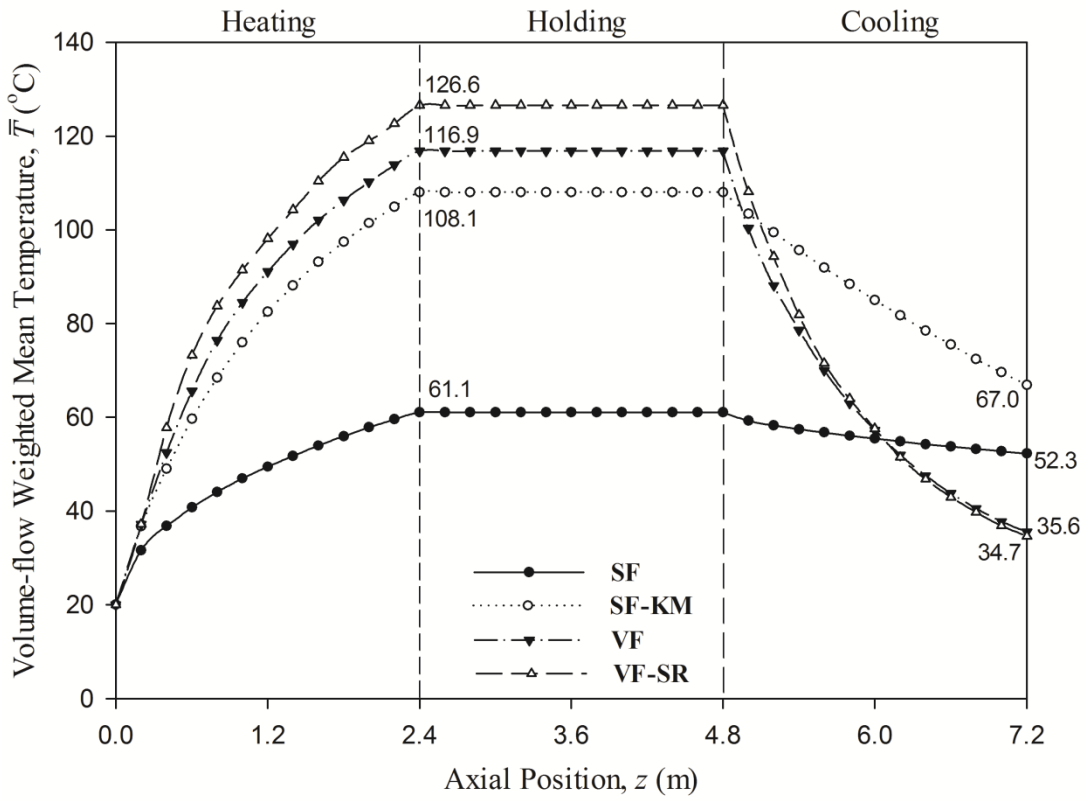

Figure 14. Development of mean temperature along heat-hold-cool process: T_w = 140 °C (heating); T_w = 20 °C (cooling).

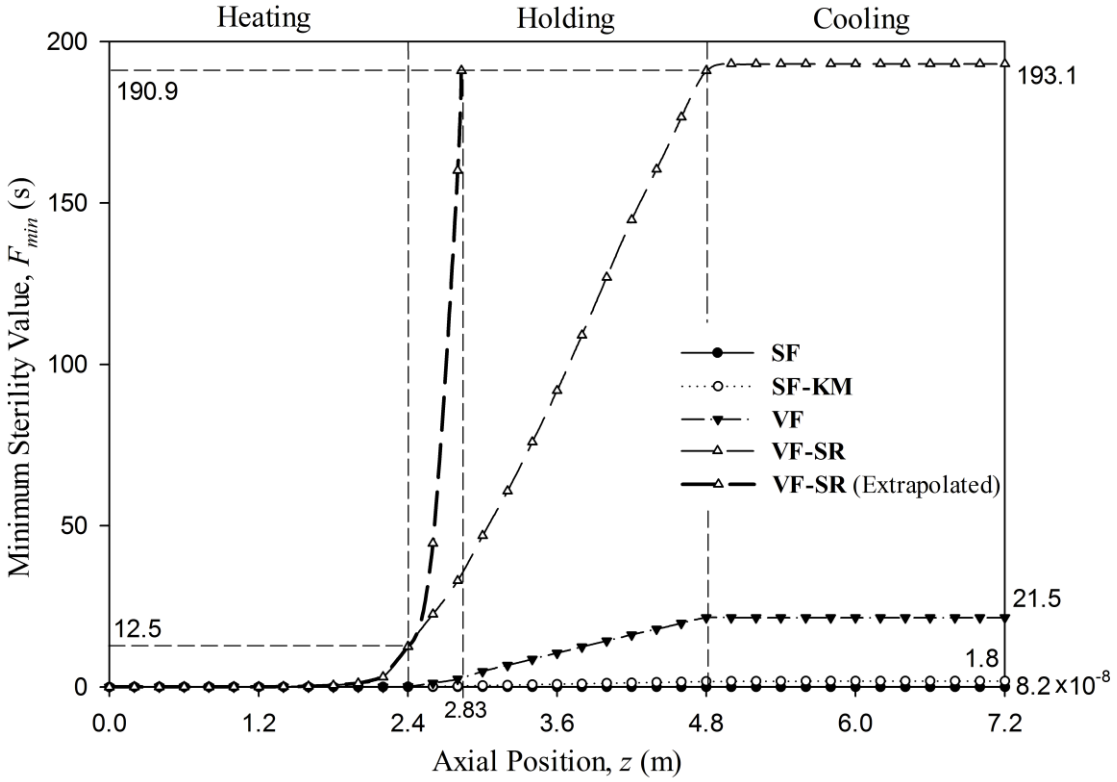

Figure 15. Development of minimum F-value along heat-hold-cool process: T_w = 140 °C (heating); T_w = 20 °C (cooling) – process axial temperature profile shown in Figure 14.

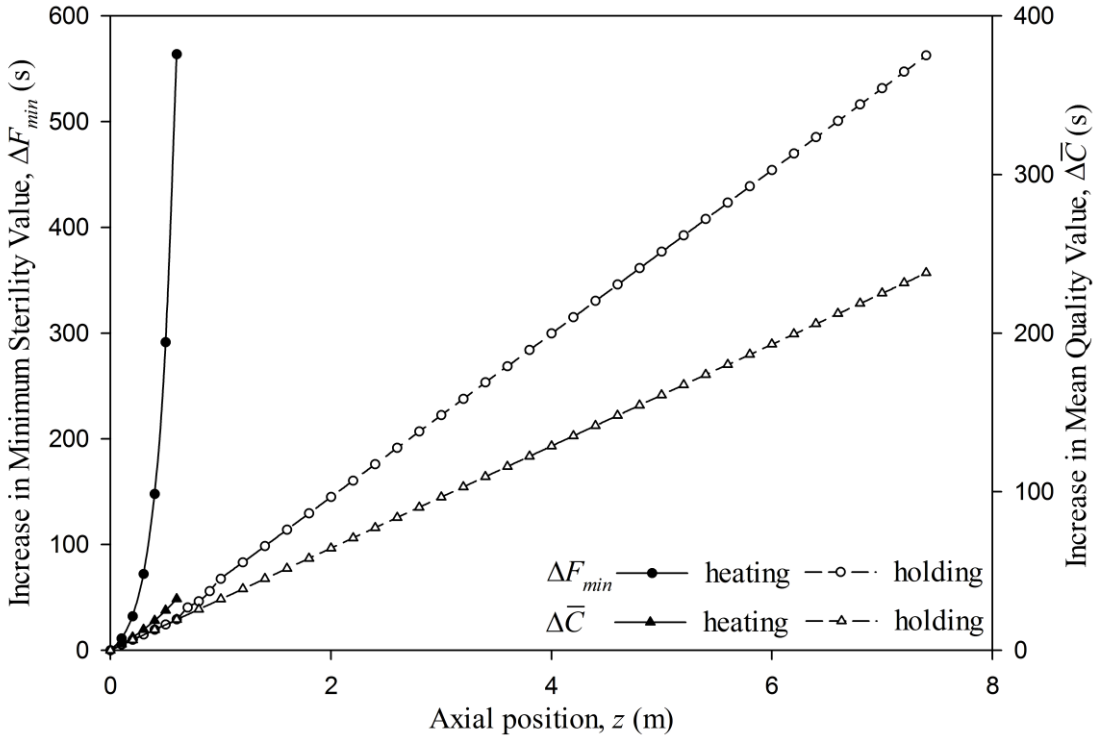

Figure 16. Increase in minimum sterility and mean quality arising from extending the **VF-SR** heating tube compared with using a **VF-SR** holding tube.

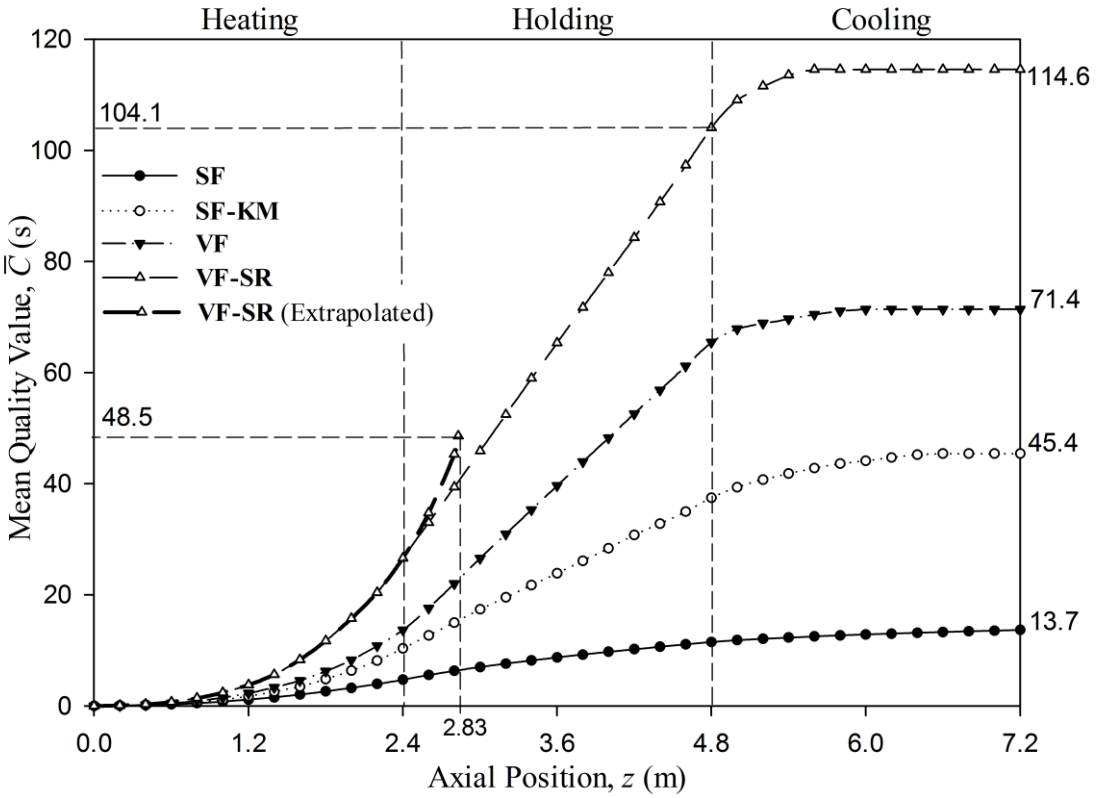

Figure 17. Development of mean C-value along heat-hold-cool process: T_w = 140 °C (heating); T_w = 20 °C (cooling) – process axial temperature profile shown in Figure 14.

Table 1: Rheological parameters used in simulations.

$\bar{w}$ (m s^{-1})	D (mm)	k_0 (Pa s)	E_a (J mol^{-1})	R_g (J mol^{-1} K^{-1})	ρ (kg m^{-3})	C_p (J kg^{-1} K^{-1})	λ (W m^{-1} K^{-1})	$\mu = k_0 exp\left(\frac{E_a}{R_g T}\right)$ (Pa s)	
								20 °C	140 °C
0.04	30	5.0×10^{-7}	35,000	8.314	998	4180	0.668	0.868	0.0134
0.04	30	5.75×10^{-6}	35,000	8.314	998	4180	0.668	10.0	0.1675

Table 2: Dimensions of Kenics static mixer (Figure 1(*b*)).

Segment length (mm)	**Gap width (mm)**	**Element length (mm)**	**Mixer diameter (mm)**	**Element thickness (mm)**	**Twist angle (rad)**
50	2.5	45	30	1	π

Table 3: Process parameters (Jung and Fryer, 1999).

Flowrate ($m^3 h^{-1}$)	**Density** ($kg m^{-3}$)	**Viscosity** (Pa s)	**Specific heat** ($J kg^{-1} K^{-1}$)	**Thermal conductivity** ($W m^{-1} K^{-1}$)	**Heating temperature** (°C)	**Cooling temperature** (°C)	**Heating length** (m)	**Holding length** (m)	**Cooling length** (m)
0.1	998	0.001	4180	0.6	140	20	12	12	12

Table 4: Mean sterility and quality in heating and cooling stages.

	Heating stage				Cooling stage			
	SF	**SF-KM**	**VF**	**VF-SR**	**SF**	**SF-KM**	**VF**	**VF-SR**
$\bar{F}$ (s)	0.32	1.73	7.15	37.59	49.53	10.87	7.70	7.35
F_{min} (s)	3.9×10^{-9}	0.086	0.13	12.5	-	-	-	-
$C_{v\text{-}F}$ (-)	3.75	1.58	1.33	1.09	0.091	0.022	0.022	0.020
$\bar{C}$ (s)	4.71	10.77	15.02	25.98	31.56	17.07	9.15	8.77
$C_{v\text{-}C}$ (-)	1.69	0.28	0.27	0.14	0.099	0.050	0.032	0.029

Table 5: Mean exit quality in heating tubes achieving the same minimum sterility at exit (F_{min} = 12.5 s).

	SF	**SF-KM**	**VF**	**VF-SR**
$\bar{C}$ (s)	505.74	44.83	33.21	25.98
$C_{v\text{-}C}$ (-)	0.96	0.32	0.16	0.14
L (m)	26.0	4.0	3.2	2.4

Table 6: Simulation parameters for complete heat-hold-cool process.

Mean velocity ($m\ s^{-1}$)	**Heating wall temperature (°C)**	**Cooling wall temperature (°C)**	**Heating length (m)**	**Holding length (m)**	**Cooling length (m)**
0.04	140	20	2.4	2.4	2.4

Highlights

- Chaotic viscous flow significantly improves heat transfer and temperature uniformity
- Sterility and product quality are enhanced by several orders of magnitude
- Nearly uniform sterility and quality distributions are achieved across flow
- Potential for achieving high temperature for short time (HTST) processing is significant
- A vibrated heat-hold-cool process is very short and the holding stage may be obviated